CHINESE OPTICS LETTERS

Vol. 23, No. 1 | January 2025

Dynamical tuning multifunctional and nonreciprocal polarization conversion by twisting twin Weyl-semimetal layers

Guangfan Liu (刘光帆)[1,†], Shuai Deng (邓 帅)[1,†], Sen Hong (洪 森)[1], Qiongxiong Ma (马琼雄)[2,*], Chengping Yin (尹承平)[1,3,**], and Kunyuan Xu (许坤远)[1,3,***]

[1] Key Laboratory of Atomic and Subatomic Structure and Quantum Control (Ministry of Education), Guangdong Basic Research Center of Excellence for Structure and Fundamental Interactions of Matter, School of Physics, South China Normal University, Guangzhou 510006, China

[2] Guangdong Provincial Key Laboratory of Nanophotonic Functional Materials and Devices, South China Normal University, Guangzhou 510006, China

[3] Guangdong Provincial Key Laboratory of Quantum Engineering and Quantum Materials, Guangdong-Hong Kong Joint Laboratory of Quantum Matter, South China Normal University, Guangzhou 510006, China

[†]These authors contributed equally to this work.

*Corresponding author: maqx@m.scnu.edu.cn

**Corresponding author: yinchengping1979@163.com

***Corresponding author: xuky@scnu.edu.cn

Received March 28, 2024 | Accepted July 17, 2024 | Posted Online January 27, 2025

Recently, polarization conversion based on the equivalent magnetic field of Weyl semimetals (WSMs) has gained significant attention. Based on a twin WSM-layer structure, we transplant the concept of twist from Twistronics to obtain a dynamically tunable polarization converter with multifunctions and nonreciprocity. One-way conversion of linear polarization to its orthogonal state can be obtained and tuned by twisting the converter. Moreover, nonreciprocal conversion from linear polarization to elliptical polarization (with ellipticity linearly tuned from −1 to 1 by twisting the converter) in one way and to quasi-linear polarization in the other way can be obtained. Calculations show that the converter achieves 95% efficiency, high optical isolation (100 dB), and low insertion loss (<2 dB). The proposal may find applications in tunable and nonreciprocal devices for integrated photonics.

Keywords: nonreciprocity; polarization conversion; tunable; twisting; Weyl semimetals.
DOI: 10.3788/COL202523.013602

1. Introduction

Polarization, which describes the oscillation direction of the electric field and indicates the transverse nature of light, is one of the fundamental properties of electromagnetic waves[1,2]. Polarization plays an important role in signal transmission and optoelectronic sensing, particularly in wireless communication and imaging, which are closely related to polarization conversion[3,4]. Therefore, the research significance of electromagnetic wave polarization conversion becomes particularly important. Traditional polarization conversion is usually achieved using birefringent materials or materials based on the Faraday effect[5]. However, due to their complexity, limited functionality, and large volume, further development and practical applications are restricted. With the progress of research, the development of multifunctional polarization converters using metamaterials or metasurfaces has attracted widespread attention[6–8]. Nevertheless, challenges still exist, such as severe losses, lack of tunability, and narrow working bandwidth, which limit the conversion efficiency and working frequency of the devices. Therefore, there is an urgent need to explore better alternative solutions.

In recent years, Weyl semimetals (WSMs) have attracted significant attention due to their unique and interesting optical properties exhibited in their band structures[9–13], such as chiral anomaly[14,15] and the anomalous Hall effect[16]. WSMs have an even number of Weyl nodes in their band structure, each carrying a quantized topological charge[17]. WSMs arise when the reversal of either parity (P) or time-reversal (T) symmetry is broken, leading to the appearance of Weyl nodes[18]. Weyl nodes in WSMs act as sources or sinks of Berry curvature, playing the role of equivalent magnetic charges in momentum space[19]. Due to the presence of the equivalent magnetic field, the dielectric tensor of WSMs possesses nonzero off-diagonal components,

resulting in Voigt or Faraday effects[20]. Compared to traditional magneto-optical materials, WSMs exhibit significant nonreciprocity without the need for an external magnetic field. This significant nonreciprocity is caused by the anomalous Hall effect[12]. It is worth noting that the nonreciprocity in WSMs can be tuned by varying the adjustable Fermi energy level and Weyl node separation[21]. Recently, the nonreciprocal behavior based on WSMs has been widely studied, including optical isolators[22], corner filters[23], nonreciprocal thermal radiation[24], and wideband circular polarizers[25], among others. The twisting method is well known for its unique characteristics in electronic and photonic systems. Chistyakov *et al.* proposed a tunable optical isolator based on Faraday-type twisted WSM[21]. However, in most of these works, the nonreciprocity is primarily observed in terms of intensity in a single mode, without further discussion on nonreciprocal polarization mode conversion; thus, the asymmetric permittivity tensor of the WSMs remains to be fully utilized. Research on nonreciprocal polarization conversion using WSMs is still lacking, and achieving efficient nonreciprocal tunable polarization converters in the mid-infrared frequency range remains a challenge.

In this work, dependent on the asymmetry of WSMs' permittivity tensor, we utilize twin WSM layers to introduce an additional degree of freedom (DOF), i.e., twist DOF. This additional DOF allows us to dynamically tune the nonreciprocal functions of the proposed structure. Our work can be divided into three aspects: (i) First, we discuss the unidirectional conversion between orthogonal linearly polarized light. Specifically, by adjusting the twist angle, we achieve high polarization conversion efficiency for forward incidence in the first operating frequency range, while exhibiting nearly zero transmittance for backward incidence. (ii) Next, we discuss the nonreciprocal conversion from linearly polarized states to elliptically polarized states. In the second operating frequency range, we realize a dynamically tunable nonreciprocal polarization conversion device that can convert light from left-handed circular polarization to linear polarization, and then to right-handed circular polarization. (iii) Finally, we further elucidate the physical mechanism of the coupling effect between the nonreciprocal polarization modes of the proposed polarization converter. Additionally, through theoretical calculations, we achieve nonreciprocal polarization conversion in the mid-infrared range with a maximum polarization conversion efficiency of up to 95% and an insertion loss below 2 dB. Our design demonstrates significant potential in optical modulation and is expected to be utilized in applications such as dynamic polarization control and switchable multifunctional integrated photonics devices.

2. Model and Theoretical Calculation Method

Figure 1(a) presents a three-layer structure comprising two layers of WSM separated by a dielectric layer. The twist tuning is achieved by fixing the leftmost WSM layer and only rotating the rightmost one (similar to wringing out a wet towel). The dielectric material is silicon monoxide (SiO) with a refractive

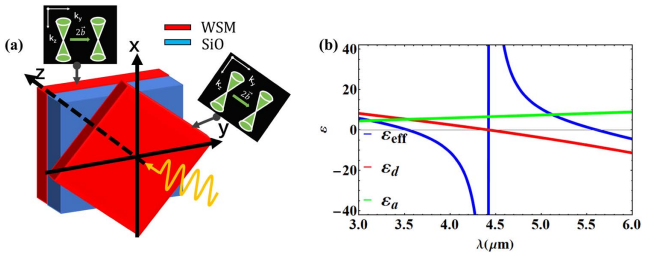

Fig. 1. Diagram of proposed structure with (a) sandwich structure composed of two layers of WSM separated by a dielectric layer and (b) wavelength dispersions of permittivity and effective permittivity.

index of 1.75[26]. The thickness of the WSM ($h_{WSM} = 300$ nm) is optimized to ensure the best nonreciprocal polarization conversion effect. The dielectric layer ($h_{SiO} = 1800$ nm) supports a Fabry–Perot resonance, concentrating the electric field primarily in this layer. This strategic arrangement effectively suppresses losses in WSM, thereby increasing the overall efficiency of the setup[21]. Figure 1(b) shows the dispersions of the permittivity and effective permittivity of WSM.

In this study, we use the magnetic WSM, which was realized experimentally using $Co_3Sn_2S_2$[13]. It has only a pair of Weyl nodes with the same energy and opposite chirality and the momentum separation is $2\vec{b}$. In the theoretical calculations, we keep the momentum separation fixed at $b = 2 \times 10^9\ \mathrm{m}^{-1}$[27]. The relative permittivity tensor of the WSM layer can be expressed as

$$\overleftrightarrow{\varepsilon} = T_z^{-1} \begin{bmatrix} \varepsilon_d & 0 & i\varepsilon_a \\ 0 & \varepsilon_d & 0 \\ -i\varepsilon_a & 0 & \varepsilon_d \end{bmatrix} T_z, \tag{1}$$

where $\varepsilon_a = \frac{e^2 b}{2\pi^2 \hbar \omega \varepsilon_0}$ and T_z is the coordinate rotational transformation matrix. The relative permittivity tensor of WSM can be obtained by the Kubo–Greenwood formula[24],

$$\varepsilon_d = \varepsilon_b + i\frac{\sigma}{\varepsilon_0 \omega}, \tag{2}$$

where ε_b and ε_0 are the background relative permittivity and vacuum permittivity, respectively, and σ is the electrical conductivity. In this study, the effective relative permittivity of the WSM layer for the transverse magnetic (TM) polarization is given by $\varepsilon_{\mathrm{eff}}^{\mathrm{TM}} = \frac{\varepsilon_d^2 - \varepsilon_a^2}{\varepsilon_d}$ and the transverse electric (TE) polarization is given by $\varepsilon_{\mathrm{eff}}^{\mathrm{TE}} = \varepsilon_d$. We also utilized the WSM parameters ($\vec{b}$, ε_a, and σ) obtained from Ref. [27].

The Berreman matrix[28] is a useful tool for investigating the optical properties of one-dimensional (1D) structures. It is based on the solutions of Maxwell's equations for anisotropic materials. By utilizing the tangential elements of the field vectors, Maxwell's equations can be mathematically represented,

$$\frac{\partial \boldsymbol{\psi}(z)}{\partial z} = -ik_0 \boldsymbol{D}\boldsymbol{\psi}(z), \tag{3}$$

where $k_0 = \omega/c$ and $\boldsymbol{\psi}(z) = [\ E_x \quad H_y \quad E_y \quad H_x\ ]^{\mathrm{T}}$. $\boldsymbol{D}$ is called the Berreman matrix, which can be obtained from Ref. [28].

By considering the above equation as a homogeneous system of differential equations with initial conditions, we can further obtain

$$\boldsymbol{\psi}(z) = \boldsymbol{M}\boldsymbol{\psi}(z_0), \tag{4}$$

where $\boldsymbol{M} = \exp[-ik_0\boldsymbol{D}(z - z_0)]$. The matrix function $\boldsymbol{M}$ is referred to as the 4×4 transfer matrix. Then, we set the parameters of the incident media vectors $\boldsymbol{\psi}(z_0)$ and exit media vectors $\boldsymbol{\psi}(z)$, and substitute them into Eq. (4) to solve for the transmittance of TE and TM modes (T_{TE} and T_{TM}), as well as the reflectance of TE and TM modes (R_{TE} and R_{TM}) and the ellipticity ϕ_e. The polarization conversion ratio (PCR) is

$$\mathrm{PCR} = \frac{T_{\mathrm{TE}}}{T_{\mathrm{TM}} + T_{\mathrm{TE}}}. \tag{5}$$

The data presented in this paper were obtained through calculations performed using MATLAB.

3. Results and Discussions

3.1 Unidirectional conversion between orthogonal linear polarizations

When TM waves propagate from the forward ($+z$) and backward ($-z$) directions, respectively, into the proposed sandwich structure, the calculated forward and backward TM-to-TM polarization transmittance ($T^{\pm}_{\mathrm{TM}\to\mathrm{TM}}$, superscript "+" and "−" represent forward and backward, respectively); the coupled TM-to-TE polarization transmittance ($T^{\pm}_{\mathrm{TM}\to\mathrm{TE}}$) as functions of the twist angle and wavelength are shown in Fig. 2. We observed obviously nonreciprocal polarization conversion for TM-to-TE within the two spectral bands of 4.0–4.5 μm (the first band inside the white dashed frame) and 5.1–5.7 μm (the second band inside the black dashed frame) in Figs. 2(a) and 2(b). In contrast, a phenomenon for TM-to-TM seems almost reciprocal within the same two spectral bands (inside the white and black dashed frame) in Figs. 2(c) and 2(d). Furthermore, both forward and backward TM-to-TM polarization transmittance ($T^{\pm}_{\mathrm{TM}\to\mathrm{TM}}$) remain close to 0 within the white dashed frame. That is, in the first band, if the forward input is in TM mode, the output is only in TE mode, and the backward input is totally blocked. This means we can achieve unidirectional polarization conversion from TM to TE polarization in the first band. More importantly, the efficiency of this unidirectional polarization conversion can be dynamically tuned by twisting the twin WSM layers [transmittance changes with the twist angle as shown in the white dashed frame of Fig. 2(a)].

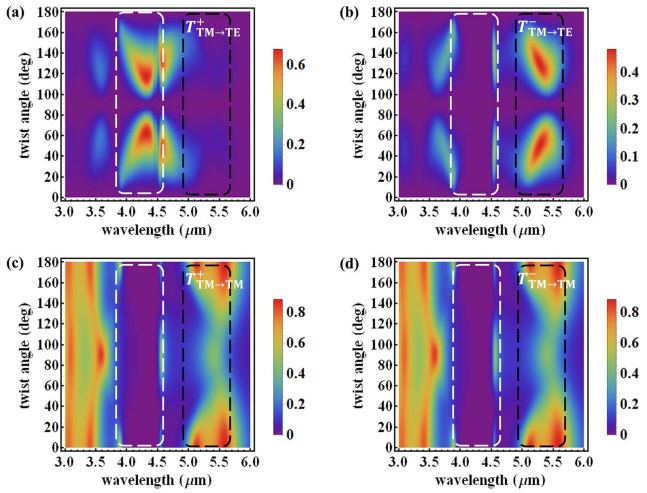

Fig. 2. Contours of the transmittance of the proposed structure as a function of twist angle and wavelength. (a) and (b) represent the transmittance of light from TM to TE polarization in the forward and backward incidence, respectively. (c) and (d) represent the transmittance of light from TM to TM polarization in the forward and backward incidence, respectively.

3.2 Nonreciprocal conversion of light from linear to elliptical polarization

There is a difficulty in analyzing the simultaneous existence of two types of polarized light, thus necessitating the introduction of ellipticity. When the ellipticity is ±1, the light is considered as left/right circularly polarized light. When the ellipticity is close to 0, the light can be considered as quasi-linear polarized light. As shown in Fig. 3, we have plotted the function of ellipticity with respect to the twist angle and wavelength. It is worth noting that in Figs. 3(a) and 3(b), there is an occurrence of opposite rotation of elliptically polarized light for both forward and backward incidence in the range of 4.5 to 5.3 μm. A particular nonreciprocal phenomenon is observed at the positions encircled by

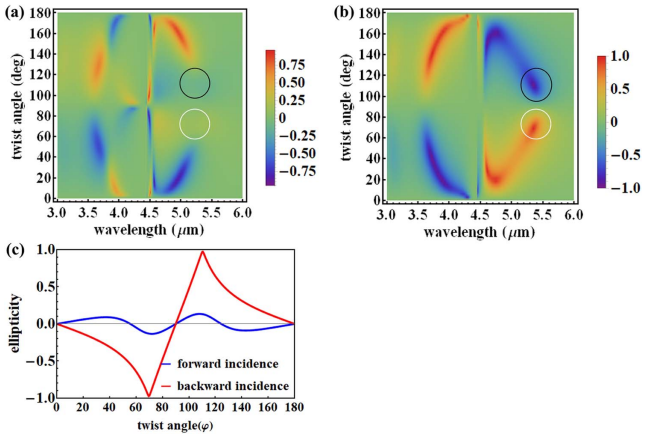

Fig. 3. Contours of the ellipticity as a function of twist angle and wavelength. (a) is for the forward incidence, and (b) is for the backward incidence. (c) The relationship between the twist angle and ellipticity for forward (blue line) and backward (red line) incidences at the wavelength of 5.36 μm.

the black and white frames: for forward incidence, the outgoing light remains as quasi-linear-polarized light, while for backward incidence, the outgoing light is circularly polarized light. In order to further visualize this phenomenon, we calculated the relationship between the ellipticity and twist angle at a wavelength of 5.36 μm, as shown in Fig. 3(c). During the process of twisting the twin WSM layers from 70° to 110°, the forward incident light results in output with quasi-linear polarization, while the backward incident light results in output with ellipticity linearly changing from −1 (right-handed circular polarization) to 0 (linear polarization), and then to +1 (left-handed circular polarization). In other words, by twisting the WSM structure, we can not only achieve nonreciprocal polarization conversion from TM polarization to TE polarization but also enable nonreciprocal polarization conversion for rich types of polarizations.

3.3 Physical mechanism and parameter analysis

To further reveal the reasons for the nonreciprocal polarization conversion, it is necessary to clarify the optical properties of a single WMS layer. Figure 4 illustrates the contours of transmittance and reflectance of a nonrotating single-layer WSM structure as functions of incident angle and wavelength for TE [Figs. 4(a) and 4(b)] and TM [Figs. 4(c) and 4(d)] polarizations, respectively. For the TE-polarized light, a transmittance plateau with a value near 1 (so that the corresponding reflectance is almost zero) emerges within the first band with wavelengths of 4.0 to 4.5 μm. In contrast, for TM-polarized light, the phenomenon is the opposite, with a reflectance plateau and almost no transmission in the same wavelengths. The reason for this phenomenon is that the effective dielectric function $\varepsilon_{\mathrm{eff}}^{\mathrm{TM}}$ for TM polarization undergoes a sharp and significant jump near 4.4 μm, with a large numerical value. As a result, it leads to a high effective refractive index resulting in a low transmittance. On the other hand, the effective dielectric function $\varepsilon_{\mathrm{eff}}^{\mathrm{TE}}$ for TE polarization is zero near 4.4 μm, resulting in a high transmittance peak[29]. At this moment, the single-layered WSM structure acts as a TE polarizer within this wavelength range. As the wavelength increases, the effective dielectric function $\varepsilon_{\mathrm{eff}}^{\mathrm{TM}}$ for TM polarization reduces to zero near 5.6 μm, resulting in a zero effective refractive index. Therefore, a high transmittance peak occurs in this wavelength range. On the other hand, the effective dielectric function $\varepsilon_{\mathrm{eff}}^{\mathrm{TE}}$ for TE polarization gradually increases, leading to a continuous decrease in transmittance. Therefore, within the wavelength range of 5.1 to 5.7 μm, we can consider the single-layer WSM structure as a TM polarizer.

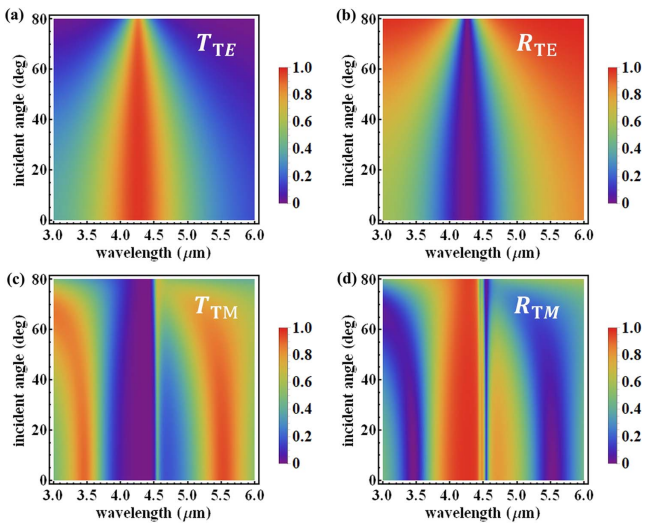

Fig. 4. Contours of the transmittance and reflectance as a function of incident angle and wavelength. In (a) and (b), the transmittance and reflectance of an incident TE-polarized light on the nonrotating single-layer WSM are represented, respectively. Similarly, in (c) and (d), the transmittance and reflectance of an incident TM-polarized light are represented.

To clarify the nonreciprocal mechanism, we have included Fig. 5 for illustration. As shown in Fig. 5(a), the fixed (nonrotated) WSM layer in the three-layer structure functions as a TE polarizer in the 4.0 to 4.5 μm spectral range. For forward incidence, the TM light first enters the rotated WSM layer. Due to the polarization mode coupling originally for the asymmetry of the WMS, the outgoings are TM and TE modes. Then the mixing modes enter the fixed WSM layer by acting as a TE polarizer, which results in the conversion of TM polarization into TE polarization. On the other hand, for backward incidence, TM-polarized light cannot pass through the fixed WSM layer. This leads to a unidirectional orthogonal linear polarization conversion. As shown in Fig. 5(b), the fixed WSM layer in the 5.1 to 5.7 μm spectral range functions as a TM polarizer. For forward incidence, the TM light initially generates both TM-polarized and TE-polarized lights under the influence of the rotated WSM layer. However, most of the TE-polarized light cannot pass through the fixed WSM layer, resulting in outgoing light with quasi-TM polarization. On the other hand, for backward incidence, the TM light can pass through the fixed WSM

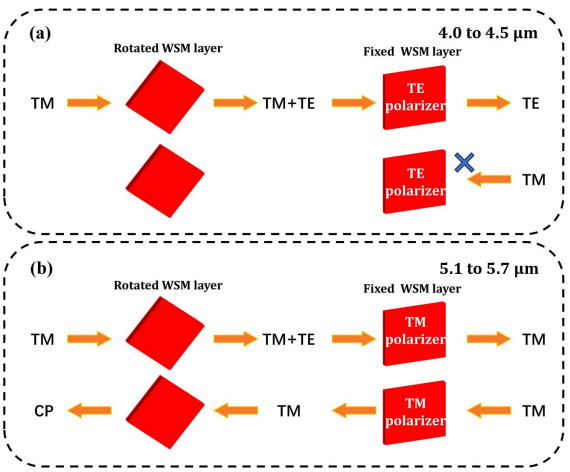

Fig. 5. Explanations of unidirectional conversion between (a) orthogonal linear polarizations and (b) nonreciprocal conversion of light from linear to elliptical polarization.

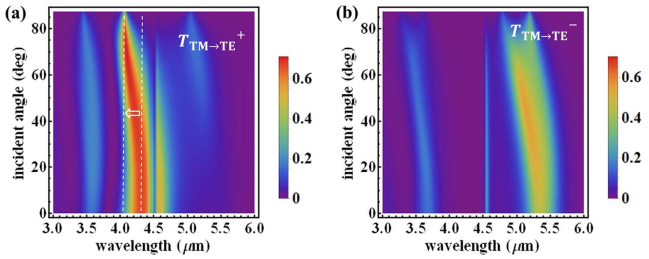

Fig. 6. Contours of the transmittance of the proposed structure as a function of incident angle and wavelength, in which twist angle $\varphi = 120°$. (a) and (b) represent the transmittance of TM-to-TE polarization light in the forward and backward cases, respectively.

layer and generate circularly polarized light under the influence of the rotated WSM layer, thereby enabling nonreciprocal polarization conversion.

In order to further show the performance of the proposed structure, we fixed the twist angle at 120°. As depicted in Fig. 6, we observed nonreciprocal phenomena even at large incident angles within the wavelength ranges of 4.0 to 4.5 μm and 5.1 to 5.7 μm. Furthermore, as the incident angle increases, a blueshift occurs for the nonreciprocal band. This shift is indicated by the movement of the band center from the right white dashed line (for 0° incident angle) to the left one (for 85° incident angle) in Fig. 6(a).

In terms of other performance properties, the results shown in Figs. 7(a) and 7(b) demonstrate that in the wavelength range of 4.0 to 4.5 μm, the incident light from the front exhibits a polarization conversion rate of over 95%, which is significantly greater than the polarization conversion rate of the light incident from the rear. Figure 7(c) shows that within the wavelength range of 4.1 to 4.5 μm, the optical isolation coefficient of the structure can be maintained at over 20 dB, reaching up to nearly 100 dB, while the insertion loss remains below 2 dB. This indicates that the

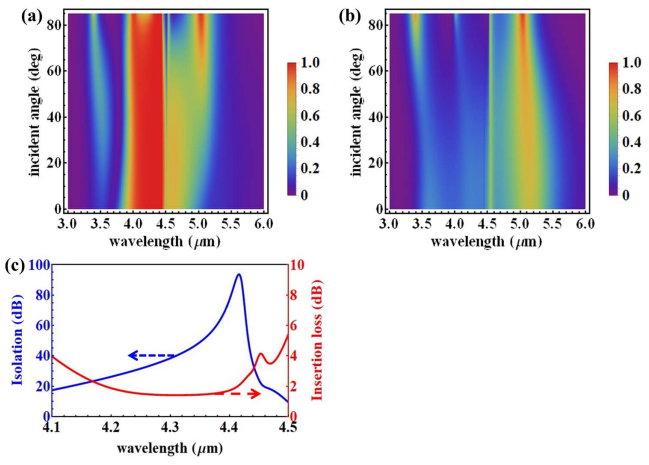

Fig. 7. Contours of the polarization conversion rate as a function of incident angle and wavelength, in which twist angle $\varphi = 120°$. (a) is for the forward incidence and (b) is for the backward incidence. (c) Isolation loss and insertion loss as a function of wavelength.

Table 1. Comparison of the Performance of Various Optical Polarization Converters.

	PCR	ISO (dB)	Band range (μm)	Thickness
Conventional optical components[30]	>90%	10–30	0.4–0.6	About 1 cm
Ours	>95%	20–100	4.1–4.5	2 μm

structure can work as a polarization converter with an additional effective isolating function. It is noteworthy that the thickness of the proposed structure is a subwavelength of approximately 0.56λ. From Table 1, we can see that although our structure is similar to the functionality achieved by conventional optical components like wave plates and polarizers[30], compared to them, our proposed structure stands out due to its significantly reduced thickness (only 0.56λ) and higher isolation (up to 100 dB). These advantages are pivotal in advancing the development of more compact optical devices.

It should be pointed out that although our work is purely theoretical work, the versatile polarization converter achieved in our work can potentially be realized in experiments. This three-layer structure, composed of two layers of WSM, can be fabricated using magnetron sputtering technology[31].

4. Conclusion

In conclusion, we propose a new method for dynamically tuning nonreciprocal polarization conversions based on twisting twin WSM layers. Introducing the twist concept not only enriches the phenomena of the polarization conversion but also makes the converter dynamically tunable. By adjusting the twist angles of the WSM layers, different nonreciprocal polarization conversions can be realized in two operating wavebands. It is worth noting that the Fermi level (E_F) of WSMs can be modified through various methods, such as chemical doping[32] and temperature variation[12]. The change in the Fermi level influences the frequency band of dielectric function transitions, thereby enabling control of this characteristic across different operational frequency bands. Simultaneously, increasing the momentum separation size $\vec{b}$ in WSM is equivalent to increasing the effective magnetic field, which helps to broaden the operational bandwidth of nonreciprocal polarization. With the development of WSMs, it is expected that WSMs with larger momentum separation will be fabricated in the future, aiding the proposed structure in achieving a wider nonreciprocal operational bandwidth. In the model of WSMs studied in this paper, within the first waveband, the structure enables unidirectional polarization conversion between orthogonal linearly polarized lights. In the second waveband, when the structure is illuminated with backward incident light, it can convert linearly polarized light into left/right circularly polarized light while maintaining linearly polarized output for forward incident light. This provides new possibilities for tunable polarization manipulation.

Furthermore, we reveal the fundamental principles of this polarization transformer through the design asymmetry of the structure. It is worth noting that this structure has a very thin thickness (only 0.56λ), and it can achieve maximum isolation of nearly 100 dB with insertion loss as low as 2 dB. This design offers advantages such as dynamical tunability, high isolation, absence of external magnetic fields, and compact size. It surpasses other methods based on magneto-optics or time modulation effects and holds great potential for precise control and regulation of light, providing new insights for the design and application of optical devices.

Acknowledgements

This work was supported by the Guangdong Provincial Key Laboratory (No. 2020B1212060066).

References

1. A. H. Dorrah, N. A. Rubin, A. Zaidi, *et al.*, "Metasurface optics for on-demand polarization transformations along the optical path," Nat. Photonics **15**, 287 (2021).
2. N. K. Grady, J. E. Heyes, D. R. Chowdhury, *et al.*, "Terahertz metamaterials for linear polarization conversion and anomalous refraction," Science **340**, 1304 (2013).
3. N. Moroney, L. Del Bino, S. Zhang, *et al.*, "A Kerr polarization controller," Nat. Commun. **13**, 398 (2022).
4. I. S. Osborne, "A metasurface polarization camera," Science **365**, 40 (2019).
5. Z. Cai, Y. Ding, Z. Chen, *et al.*, "Dynamic dual-functional optical wave plate based on phase-change meta-molecules," Opt. Lett. **48**, 3685 (2023).
6. Y. Deng, C. Wu, C. Meng, *et al.*, "Functional metasurface quarter-wave plates for simultaneous polarization conversion and beam steering," ACS Nano **15**, 18532 (2021).
7. X. Shi, Y. Lu, and H. Ou, "High-performance silicon carbide polarization beam splitting based on an asymmetric directional couplers for mode conversion," Opt. Lett. **48**, 616 (2023).
8. J. Liu, D. Zhang, Q. Wen, *et al.*, "Tunable linear-to-circular terahertz polarization convertor enabled by a plasmonic nanocomposite metasurface," Opt. Express **31**, 39557 (2023).
9. Z. Tan, F. Fan, D. Zhao, *et al.*, "Nonreciprocal terahertz beam steering manipulated by magnetic Weyl semimetal metasurface based on universal chirality-wavevector-magnetic field relation," Laser Photonics Rev. **18**, 2301008 (2023).
10. D. F. Liu, A. J. Liang, E. K. Liu, *et al.*, "Magnetic Weyl semimetal phase in a Kagomé crystal," Science **365**, 1282 (2019).
11. C. Zhao, G. Hu, Y. Chen, *et al.*, "Unidirectional bound states in the continuum in Weyl semimetal nanostructures," Photonics Res. **10**, 1828 (2022).
12. C. Guo, V. S. Asadchy, B. Zhao, *et al.*, "Light control with Weyl semimetals," eLight. **3**, 2 (2023).
13. Y. Okamura, S. Minami, Y. Kato, *et al.*, "Giant magneto-optical responses in magnetic Weyl semimetal $Co_3Sn_2S_2$," Nat. Commun. **11**, 4619 (2020).
14. P. Kim, J. H. Ryoo, and C.-H. Park, "Breakdown of the chiral anomaly in Weyl semimetals in a strong magnetic field," Phys. Rev. Lett. **119**, 266401 (2017).
15. S. Howard, L. Jiao, Z. Wang, *et al.*, "Evidence for one-dimensional chiral edge states in a magnetic Weyl semimetal $Co_3Sn_2S_2$," Nat. Commun. **12**, 4269 (2021).
16. E. Liu, Y. Sun, N. Kumar, *et al.*, "Giant anomalous hall effect in a ferromagnetic Kagome-lattice semimetal," Nat. Phys. **14**, 1125 (2018).
17. K. Kuroda, T. Tomita, M.-T. Suzuki, *et al.*, "Evidence for magnetic Weyl fermions in a correlated metal," Nat. Mater. **16**, 1090 (2017).
18. S. Murakami, "Phase transition between the quantum spin Hall and insulator phases in 3D: emergence of a topological gapless phase," New J. Phys. **9**, 356 (2007).
19. P. Hosur, S. A. Parameswaran, and A. Vishwanath, "Charge transport in Weyl semimetals," Phys. Rev. Lett. **108**, 046602 (2012).
20. K. Halterman, M. Alidoust, and A. Zyuzin, "Epsilon-near-zero response and tunable perfect absorption in Weyl semimetals," Phys. Rev. B **98**, 085109 (2018).
21. V. A. Chistyakov, V. S. Asadchy, S. Fan, *et al.*, "Tunable magnetless optical isolation with twisted Weyl semimetals," Nanophotonics **12**, 3333 (2023).
22. V. S. Asadchy, C. Guo, B. Zhao, *et al.*, "Sub-wavelength passive optical isolators using photonic structures based on Weyl semimetals," Adv. Opt. Mater. **8**, 2000100 (2020).
23. R. Zhang, G. Liu, S. Hong, *et al.*, "Sharp angular and unidirectional filter based on accidental degeneracy between two twisted Weyl semimetal-based defect modes in a one-dimensional photonic crystal," Opt. Lett. **48**, 3527 (2023).
24. J. Wu, B. Wu, Z. Wang, *et al.*, "The enhanced nonreciprocal radiation with topological interface states," Opt. Laser Technol. **158**, 108907 (2023).
25. C. Yang, B. Zhao, W. Cai, *et al.*, "Mid-infrared broadband circular polarizer based on Weyl semimetals," Opt. Express **30**, 3035 (2022).
26. E. D. Palik, *Handbook of Optical Constants of Solids* (Academic, 1998).
27. M. Luo, Y. Xu, Y. Xiao, *et al.*, "Strong nonreciprocal thermal radiation by optical Tamm states in Weyl semimetallic photonic multilayers," Int. J. Therm. Sci. **183**, 107851 (2023).
28. D. W. Berreman, "Optics in smoothly varying anisotropic planar structures: Application to liquid-crystal twist cells*," J. Opt. Soc. Am. **63**, 1374 (1973).
29. J. Luo, P. Xu, H. Chen, *et al.*, "Realizing almost perfect bending waveguides with anisotropic epsilon-near-zero metamaterials," Appl. Phys. Lett. **100**, 221903 (2012).
30. H. L. Gevorgyan, A. A. Rangelov, and N. V. Vitanov, "Broadband composite nonreciprocal polarization wave plates and optical isolators," Opt. Commun. **549**, 129884 (2023).
31. K. Fujiwara, J. Ikeda, J. Shiogai, *et al.*, "Ferromagnetic $Co_3Sn_2S_2$ thin films fabricated by co-sputtering," Jpn. J. Appl. Phys. **58**, 050912 (2019).
32. V. Rai, S. Jana, J. Perbon, *et al.*, "Weyl points and anomalous transport effects tuned by the Fe doping in Mn_3Ge Weyl semimetal," New J. Phys. **26**, 033043 (2024).